Acta Chemica Scandinavica, 1997: 51: 504–514
Printed in UK – all rights reserved

ACTA
CHEMICA SCANDINAVICA
ISSN 0904–213X

Solubility of MgO in Mixed Chloride–Fluoride Melts Containing $MgCl_2$

Heidi Mediaas, Jens Emil Vindstad and Terje Østvold*

Institute of Inorganic Chemistry, Norwegian University of Science and Technology, N-7034 Trondheim, Norway

Mediaas, H., Vindstad, J. E. and Østvold, T., 1997. Solubility of MgO in Mixed Chloride–Fluoride Melts Containing $MgCl_2$. – Acta Chem. Scand. 51: 504–514.

The effect on MgO solubility of fluoride additions to $MgCl_2$-containing melts has been studied. An almost linear increase in MgO solubility as function of MgF_2 mole fraction was observed in $MgCl_2$–MgF_2 melts at 840 °C. In pure $MgCl_2$ the MgO saturation mole fraction was determined to be $x^{sat}_{MgO} = 0.0061 \pm 0.0002$ at 840 °C in the $MgCl_2$–MgF_2 ($x_{MgF_2} = 0.40$) mixture to $x^{sat}_{MgO} = 0.0109 \pm 0.0002$ at 840 °C.

The effect of temperature on the MgO solubility was determined for pure $MgCl_2$ and for two $MgCl_2$–MgF_2 mixtures ($x_{MgF_2} = 0.1816$ and $x_{MgF_2} = 0.2016$): $d(\ln x^{sat}_{MgO})/d(1/T)$ was -5200 K for $MgCl_2$ and -4200 K for the two mixtures, respectively. Three different oxide solubility experiments were performed for the $MgCl_2$–NaCl–NaF ternary: 1. NaF and $MgCl_2$ were added to a NaCl–$MgCl_2$ mixture saturated with MgO at 850 °C such that $x_{MgCl_2} = 0.63$. The MgO solubility increased with NaF content up to $x_{NaF} \approx 0.08$, whereafter it was constant to $x_{NaF} = 0.20$. 2. NaF was added to a NaCl–$MgCl_2$ mixture saturated with MgO at 850 °C. $x^{\circ}_{MgCl_2} = 0.63$ was the initial $MgCl_2$ concentration. An increase in MgO solubility up to about 8 mol% NaF was observed. On further NaF additions to $x_{NaF} = 0.18$ the MgO solubility decreased. 3. A melt closer in composition to the electrolyte used for electrowinning of magnesium was investigated. The $MgCl_2$ mole fraction was kept constant at $x_{MgCl_2} = 0.10$. The temperature was 900 °C. No effect of NaF content on the MgO solubility could be observed for $x_{NaF} \leq 0.06$.

The specific energy consumption for electrolytic magnesium metal production for a given cell may be calculated from eqn. (1)

$$N = V/0.454\eta \quad (1)$$

where N is the specific energy [in kW h $(kgMg)^{-1}$], V the electrolyser voltage (in V), and η is the current efficiency. Today the energy consumption is about 13–14 kW h per kgMg, a reduction of more than 6 kW h since the early days of the art.[1] However, the thermodynamic energy required is only about 6.8 kW h per kgMg at 700 °C,[2] and it may therefore still be possible to cut the energy consumption considerably. Physicochemical properties such as density,[3,4] conductivity[5] and viscosity[6] of the electrolyte, and interfacial tensions[7–11] between the Mg metal pool, the atmosphere, the melt and the steel cathode are of significant importance for the current and energy efficiencies. A high current efficiency requires that the cathode is well wetted by the liquid magnesium and that the latter is well wetted by the electrolyte.[12] Oxide impurities may form a passivating layer on the cathode surface,[13] and may also concentrate on the surface of Mg droplets in such a way that these droplets become dispersed in the melt instead of coalescing with the Mg pool.[12] One way to increase the energy efficiency will thus be to obtain better control over the oxide and hydroxide species dissolved in the bath.

Fluoride additions in the form of NaF or CaF_2 to $MgCl_2$–NaCl melts have been reported to improve the technical electrolysis of magnesium if the $MgCl_2$ feed contains oxide impurities.[12,14] Additions of AlF_3, $AlCl_3$, and cryolite have also been found to have positive effects on the wettability of the cathode by magnesium, on the separation of the metallic magnesium from the electrolyte, and on the current efficiency. However, as Al-containing additions result in contamination of the produced metal by aluminium, such additives should be avoided.[12] For the Dow process, Rao[14] found a maximum current yield with fluoride additions corresponding to 1.0–1.4 wt% CaF_2. He attributed the beneficial effect of fluoride to its fluxing action on the surface oxide on the produced magnesium (especially the Mg droplets), leading to increased rate of coalescence of small magnesium droplets dispersed in the melt. Another reason for the increased current efficiency observed by Rao may be

* To whom correspondence should be addressed.

that fluorides enhance the surface tension of the electrolyte at the boundary between the fused magnesium and the solid cathode, thereby favouring the persistence and growth of magnesium metal on the cathode.[12] Extensive investigations recently performed in a Mg smelter fed with anhydrous $MgCl_2$ showed no increase in oxide contents in the bath when CaF_2 was added to the electrolyte.[15] The same experiment did not reveal any positive correlation between the fluoride content of the electrolyte and the current efficiency for that smelter.

Only a few papers addressing the solubility of MgO in $MgCl_2$-containing halide melts have been published.[16–19] Sharma[17] measured the MgF_2-rich side of the MgF_2–MgO binary phase diagram by differential thermal analysis. A eutecticum was found at 8.5 mol% MgO and 1228 °C, and a steep MgO liquidus line was indicated. Boghosian and co-workers[18] found the solubility of MgO to increase with increasing x_{MgCl_2} in the system NaCl–$MgCl_2$, up to 0.36 mol% in pure $MgCl_2$ at 730 °C. They observed no effect of temperature on the MgO solubility up to 830 °C for $0.5 < x_{MgCl_2} < 0.75$. It was, therefore, reasonable to assume that the oxide solubility of a $MgCl_2$-containing melt should increase with increasing F^- content of the melt. This was also confirmed by Mediaas *et al.*[19]

Combes *et al.*[16] performed potentiometric titrations of equimolar NaCl–KCl melts containing small amounts of $MgCl_2$ with BaO. They reported the existence of a stable oxide complex $Mg_2OCl_x^{2-x}$. The existence of this complex was later confirmed by Boghosian *et al.*,[18] who investigated the solubilities of MO in MCl_2–NaCl melts (M = Mg, Ca, Sr and Ba). The solubility of each alkaline earth oxide was strongly dependent on the activity of the corresponding chloride. The activity coefficient of Mg_2OCl_2 was found to be independent of the $MgCl_2$–NaCl composition both for $x_{MgCl_2} \leqslant 0.33$ and $x_{MgCl_2} \geqslant 0.33$, respectively.

There is a need to understand the role of NaF additions to the technical melt mixtures used during Mg production. We therefore decided to study the effect of NaF on the MgO solubility since NaF seems to have a positive influence on cell performance for some types of electrolytes. In the present study we concentrated on melts having very low moisture or oxide content. In order to achieve a deeper understanding of the mechanisms involved during dissolution of MgO in melts of the $MgCl_2$–NaCl–NaF reciprocal ternary system, it was found necessary to compare the findings from this system with results from the simpler $MgCl_2$–MgF_2 mixture, which exhibits close to ideal behaviour according to the phase diagram.[20] Therefore, the MgO solubility in the $MgCl_2$–MgF_2 system has been determined at 840 °C for MgF_2 contents up to 40 mol%. The effect of temperature on the MgO solubility was also investigated. Some of the results have been presented in a previous paper,[19] but we think the data should be reconsidered in the light of new data.

Experimental

The chemicals used were $MgCl_2 \cdot 6H_2O$ (E. Merck A.G., p.a. >99%), MgF_2 (E. Merck A.G., fibre grade), NaCl (E. Merck A.G., p.a. >99.5%), NaF (E. Merck A.G., p.a. >99%), and MgO (Fluka A.G., >97%). HCl (Messer Griesheim, 99.8%) and N_2 (Hydrogas, 99.998%) were used for the dehydration of $MgCl_2 \cdot 6H_2O$. This dehydration was done by heating $MgCl_2 \cdot 6H_2O$ from room temperature to 450 °C under a stream of HCl. The rate of heating varied from 3 to 25 °C h^{-1}, depending on temperature range and HCl flow rate. The temperature was then lowered to 100 °C, and the dehydrated chloride was flushed with N_2 for at least 24 h to remove remaining HCl. The dehydrated $MgCl_2$ was distilled under vacuum (ca. 10^{-8} bar) at about 1000 °C, and stored in sealed quartz ampoules. NaCl and NaF were dried under vacuum at 400 °C for 3–4 h, and recrystallised twice from the molten state in a platinum crucible under N_2 atmosphere. Optically pure crystals were picked and used for the experiments. MgF_2 was dried under vacuum at 400 °C for 16 h and subsequently stored in a glove box. The MgO was heated to 600 °C under vacuum for 48 h prior to use in order to decompose any remaining $MgCO_3$, and stored in a glove box.

The experimental set-up for the oxide solubility measurements is shown schematically in Fig. 1. The platinum crucible used as a melt container was filled with salts and placed at the bottom of a quartz container. The radiation shields above the Pt crucible had holes to accommodate the stirring rod, salt charger or sample

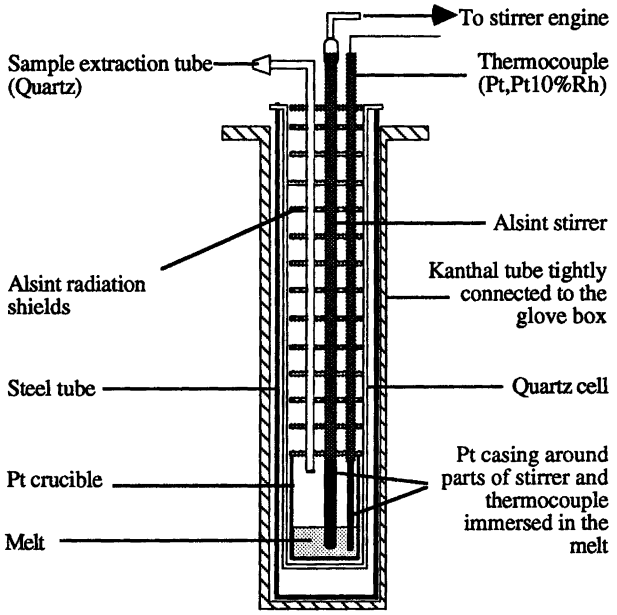

Fig. 1. Experimental set-up. The cell assembly was placed inside a vertical tube furnace connected to a glove box. A quartz sinter was attached to the lower end of the sample extraction tube. The sample extraction tube was made of graphite for the measurements with the $MgCl_2$–MgF_2 system.

extraction tube, and thermocouple. The radiation shields were mounted on Alsint (sintered alumina) rods, and separated by Alsint tubes about 2 cm long. The stirring rod was made of Alsint. The thermocouple was contained in an Alsint tube for protection, and immersed in the melt. Both the stirring rod and the thermocouple protection tube had platinum sheaths around the parts immersed in the melt. The entire cell assembly was placed inside a Kanthal tube tightly connected to a glove box. This tube was inserted into a cylindrical core of a Fibrothal RAC 100/500 wire-wound, water-cooled furnace whose temperature was controlled by a proportional controller. The cell assembly was open to the glove box argon atmosphere having a water content <1 ppm and an oxygen content <5 ppm. The sample extraction tube (quartz, 10×12 mm ϕ) had a quartz sinter of porosity 3 (pore size 15–40 μm) at the end to be immersed in the melt. This pore size is suitable for extracting samples from $MgCl_2$–NaCl melts. A syringe was attached to the other end of the sample extraction tube. For the oxide solubility measurements in the $MgCl_2$–MgF_2 melts the sampling arrangement was equal in principle to the one just described, but both the sampling tube and the filter were made from graphite.

Experimental procedure. The experiments were performed in the experimental set-up described above. For each experiment about 80–100 g of salt was used, and MgO was added in excess relative to saturation. The equilibration time for MgO dissolution was determined by measuring the oxide content of the molten mixtures as a function of time. Melt samples for analysis were withdrawn from the melt using the sampling device described above. Blind samples obtained with this sampling device from a $MgCl_2$–NaCl–NaF melt showed no additional oxide due to corrosion of the quartz filter. Samples of the fluoride–chloride melts were liquid and colourless when withdrawn from the cell, indicating that the samples were from melts above the liquidus temperature. The samples were quenched by quickly raising the sampling tube to room temperature. The sampling procedure took less than 20 s. Oxide content analyses, carbothermal reduction analysis (CR), were performed immediately after sampling. $MgCl_2$–NaCl melts were also analysed for basic O^{2-} content by the acid consumption method (AC). The oxide contents of the different $MgCl_2$–NaCl melts were compared with previous data[18] in order to check that equilibrium was established in the binary before NaF or MgF_2 was added. $MgCl_2$, MgF_2, and NaF were added through a quartz charging tube positioned just above the melt surface.

It will be noted that high oxide contents were observed for some measurements. The contaminations probably originated from $K_2S_2O_7$ which was used during a short period to clean the equipment between experiments.

The oxide analysis techniques used were carbothermal reduction using a Leco TC-436 oxygen and nitrogen determinator, CR and AC (iodometric titration). The last of these techniques is well known.

Conventional methods for analysing oxide, such as the Karl Fischer and iodometric titration methods, can not be used for fluoride-containing melts because of the low solubility of fluorides in most solvents. The oxide content of such melt samples was therefore analysed by the CR method. Leco TC-436 is made to determine oxide contents in steel, and before we could use it for our purpose, procedures for analysing hygroscopic salt mixtures were developed. In the CR analysis the sample, kept in a tin capsule, is heated until the oxide in the sample reacts with graphite to form CO, which is oxidised to CO_2 in a CuO tower. The CO_2 thus formed is detected by IR spectroscopy at a frequency characteristic for CO_2. The detection limit and accuracy are reported to be 0.1 ppm (at 1 g sample weight) and 1% of oxide present, respectively. The Leco TC-436 will determine all the oxygen present in the system, including water absorbed on the salt, provided it forms CO by reaction with carbon at the analysis temperature, which varied in the range 750–2500 °C. Furthermore, water absorbed on a $MgCl_2$-containing sample will react with $MgCl_2$ upon heating to form MgO and MgOHCl. Consequently, it is not possible during the analysis to distinguish between the contributions from absorbed water and from oxide already present in the sample. It is therefore important to prevent the sample from absorbing moisture from the atmosphere and equipment prior to analysis. A few important precautions should be taken in order to minimise the water absorption: (i) the sample should be kept and handled in a glove box with very low water content and handled with diffusion tight gloves; (ii) equipment used for sample preparation should be heated to at least 150 °C and transferred directly to the glove box while hot; and (iii) the sample surface area should be kept as small as possible to reduce water absorption, i.e. small pieces (>20 mg) rather than powder should be analysed.

Three methods for controlling the analysis temperature, the scan, automatic, and step analyses, will be discussed. The *scan* method is normally the first to be performed on a new sample. The temperature is increased continuously at a rate set by the operator, starting and ending at preset temperatures. In this way an indication of the different oxides in the sample and their respective carbothermal decomposition temperatures are obtained. This analysis forms the basis for the temperatures to be used during the automatic and step analyses. Scan analysis has proven more reliable than the other two methods for melts having oxide-containing species with high vapour pressures. Such species may escape detection during automatic analysis. The *automatic* analysis is the simplest and fastest to perform. Only one analysis temperature is applied, and only the total oxide content is detected. The *step* analysis is best suited when different oxides are to be detected. A maximum of nine temperatures may be set by the operator. The rate of temperature increase between each temperature as well as the time at each temperature can be set independently.

Examples of the three different methods are shown in Fig. 2. The amount of oxide is calculated by an integration of the area under the relative concentration curves. Empty tin capsules, used as sample containers during analysis, are analysed in the same way as the samples, and their oxide contents are subtracted from the total oxide measured. Before each analysis the graphite crucible and powder are heated to a temperature higher than the maximum analysis temperature for 60 s or more. The temperature is then lowered to the starting analysis temperature and the sample, which has so far been contained in the loader mechanism of the instrument, is dropped into the crucible. A maximum analysis temperature of slightly above 2800 °C is offered by the instrument.

In Fig. 3 a test of the CR analysis technique is presented. Small amounts of MgO were added to a $MgCl_2$–MgF_2 mixture ($x_{MgCl_2}=0.60$) in such a way as to

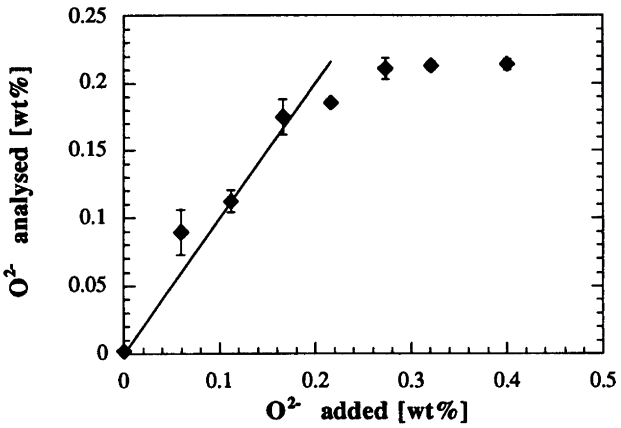

Fig. 3. Analysed versus added oxide in a $MgCl_2$–MgF_2 melt at 840 °C and $x_{MgCl_2}=0.60$. The error bars reflect the variation between parallels. (◆) experimental; (——) $wt\%O^{2-}_{anal}/wt\%O^{2-}_{add}=1$.

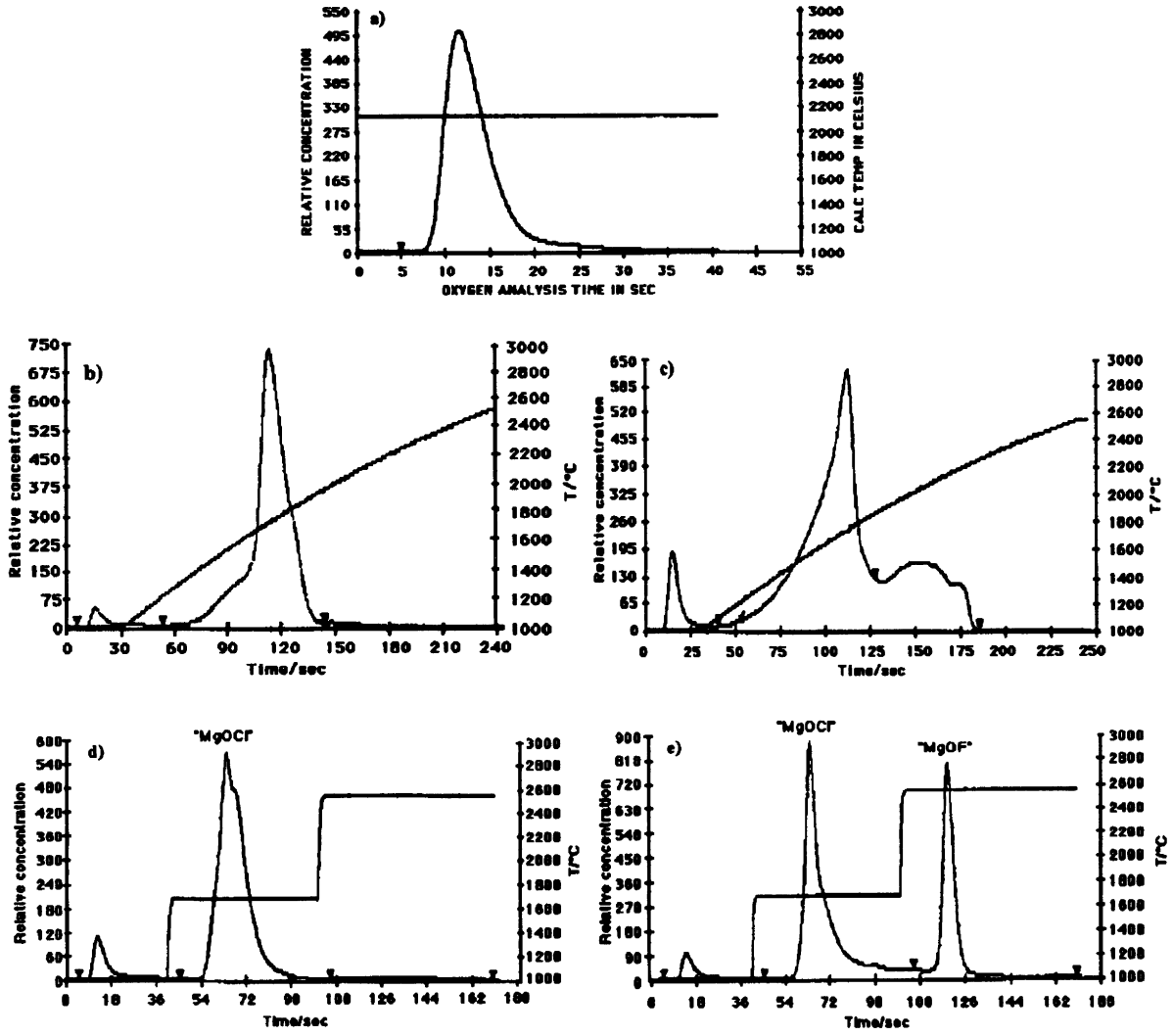

Fig. 2. MgO content in melt samples as determined by CR. (a) Automatic analysis of pure destilled $MgCl_2$ containing about 20 ppm oxide; (b) scan analysis of $MgCl_2$–NaCl–MgO; (c) scan analysis of $MgCl_2$–NaCl–NaF–MgO; (d) step analysis of $MgCl_2$–NaCl–MgO; (e) step analysis of $MgCl_2$–NaCl–NaF–MgO.

maintain a melt not saturated with MgO. Samples were withdrawn from the melt after each addition and analysed for oxide. A one-to-one relationship between added and analysed oxide content can be observed before saturation is reached. When the amount of added MgO exceeded the solubility limit, constant MgO concentrations were measured. The scatter in the results presented in Fig. 3 is mainly due to low sample weights.

Results

MgO solubilities have been determined in the $MgCl_2$–NaCl–NaF and $MgCl_2$–MgF_2 systems. Three series of experiments were performed in the $MgCl_2$–NaCl–NaF system: (i) NaF and $MgCl_2$ were added to a NaCl–$MgCl_2$ melt at 850 °C keeping $x_{MgCl_2} = 0.63$ and $x_{NaF} \leqslant 0.20$. (ii) NaF was added to a NaCl–$MgCl_2$ melt at 850 °C with an initial mole fraction of $MgCl_2$, $x^{\circ}_{McCl_2} = 0.63$. (iii) Experiment (i) was repeated with $x_{MgCl_2} = 0.10$ at 900 °C. x_{NaF} ranged from 0 to 0.10. All melts were saturated with MgO(s). Results are presented in Table 1 and in Figs. 4–6.

Two series of experiments were performed in the $MgCl_2$–MgF_2 system: (iv) MgF_2 was added to a $MgCl_2$ melt saturated with MgO at 840 °C. x_{MgF_2} ranged from 0 to 0.4. The oxide solubility in pure $MgCl_2$ was also determined using the acid consumption analysis method. Three experimental runs were performed. Results are given in Fig. 7 and in Table 2. (v) The effect of temperature on the MgO solubility in two $MgCl_2$–MgF_2 melts with $x_{MgF_2} = 0.202$ and 0.182, respectively, was investigated for $676 < T/°C < 930$. Results are given in Fig. 8 and in Table 3.

Discussion

The effect of temperature on the MgO solubility both in pure $MgCl_2$(l) and in $MgCl_2$–MgF_2 mixtures is pro-

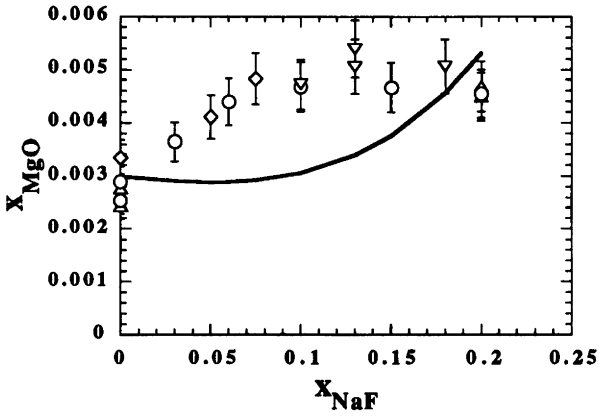

Fig. 4. Saturation mole fractions of MgO plotted versus x_{NaF} in $MgCl_2$–NaCl–NaF melts at $x_{MgCl_2} = 0.63$ and 850 °C. Different symbols indicate different experimental runs. (——) Model [eqn. (15)].

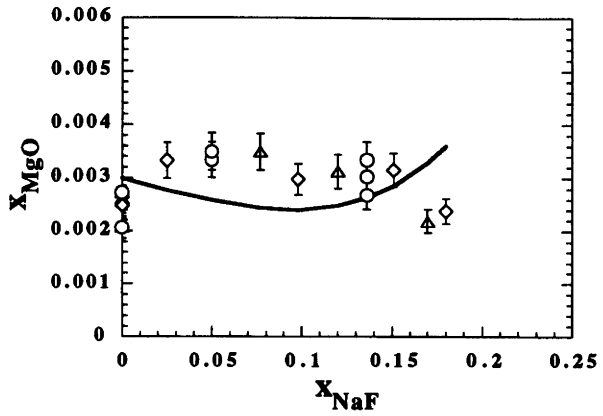

Fig. 5. Saturation mole fractions of MgO plotted versus x_{NaF} in $MgCl_2$–NaCl–NaF melts at $x_{MgCl_2} = 0.63(1\text{-}x_{NaF})$ and 850 °C. Different symbols indicate different experimental runs. (——) Model [eqn. (15)].

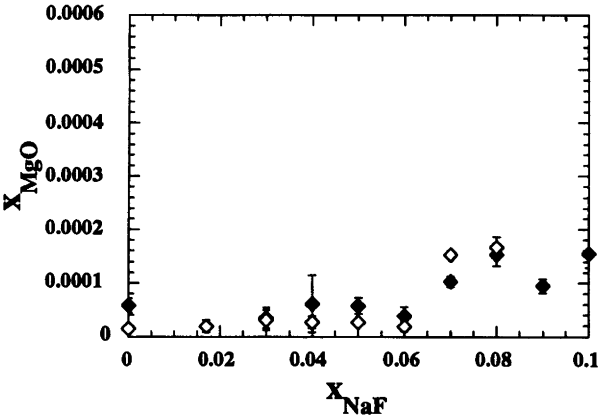

Fig. 6. Saturation mole fractions of MgO plotted versus x_{NaF} in $MgCl_2$–NaCl–NaF melts at $x_{MgCl_2} = 0.10$ and 900 °C. (◆) CR data; (◇) AC data.

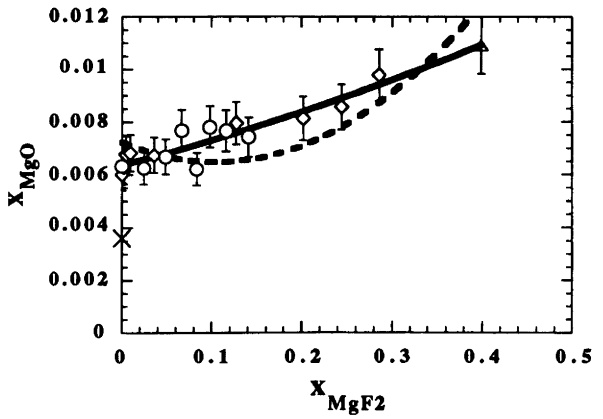

Fig. 7. MgO saturation mole fraction in the $MgCl_2$–MgF_2 binary plotted versus x_{MgF_2} at 840 °C. Different symbols indicate different experimental runs. (×) 730 °C, Ref. 18; (– – –) eqn. (15) with two parameters, K_{12} and K_{14}; (——) eqn. (15) with three parameters ($K_{12} = 0.0064$; $K_{13} = 0.021$; $K_{14} = 0.022$).

Table 1. Saturation mole fractions of MgO in $MgCl_2$–NaCl–NaF melts at 850 °C (475 °C for $x_{MgCl_2}=0.415$ and 900 °C for $x_{MgCl_2}=0.1$). Number of parallels in parentheses. Standard deviations reflect the variations between the parallels.

Melt composition			Oxide content, $x_{MgO} \times 10^3$					
			CR[a]			AC[b]		
x_{MgCl_2}	x_{NaCl}	x_{NaF}	Average		SD	Average		SD
0.63	0.37	0.0	2.5	(6)	0.3	1.71	(3)	0.04
"	"	"	3.34	(4)	0.17	2.00	(4)	0.04
"	"	"	2.8	(8)	0.3	2.24	(3)	0.02
"	0.34	0.03	3.64	(4)	0.14			
"	0.32	0.05	4.10	(4)	0.24			
"	0.31	0.06	4.39	(3)	0.19			
"	0.295	0.075	4.82	(2)	—			
"	0.27	0.10	4.67	(4)	0.09			
"	"	"	4.72	(5)	0.26			
"	0.24	0.13	5.39	(4)	0.35			
"	"	"	5.06	(4)	0.20			
"	0.22	0.15	4.66	(4)	0.25			
"	0.19	0.18	5.05	(4)	0.45			
"	"	"	5.06	(4)	0.14			
"	0.17	0.20	4.54	(5)	0.41			
"	"	"	4.48	(3)	0.24			
"	"	"	4.68	(4)	0.13			
0.63	0.37	0.00	2.3	(8)	0.4	1.2	(5)	0.1
"	"	"	2.5	(4)	0.2	1.82	(4)	0.04
"	"	"	3.0	(8)	0.4	1.6	(8)	0.2
0.614	0.361	0.025	3.33	(4)	0.20			
0.60	0.35	0.05	3.34	(5)	0.20			
"	"	"	3.49	(4)	0.28			
0.582	0.341	0.077	3.48	(4)	0.04			
0.568	0.334	0.098	2.97	(4)	0.15			
0.555	0.325	0.120	3.12	(4)	0.17			
0.545	0.319	0.136	3.03	(4)	0.08			
"	"	"	2.68	(4)	0.04			
"	"	"	3.34	(4)	0.08			
0.535	0.314	0.151	3.16	(5)	0.21			
0.523	0.307	0.17	2.18	(5)	0.08			
0.517	0.303	0.18	2.38	(4)	0.07			
0.415	0.585	0				0.43	(13)	0.03[c]
0.10	0.90	0.0	0.058	(4)	0.027	0.023	(4)	0.007
"	"	"				0.015	(3)	0.023[d]
"	0.883	0.017				0.019	(4)	0.017
"	0.87	0.03	0.035	(5)	0.038			
"	"	"				0.031	(4)	0.039[d]
"	0.86	0.04	0.061	(5)	0.108			
"	"	"				0.027	(4)	0.023[d]
"	0.85	0.05	0.058	(4)	0.031			
"	"	"				0.027	(4)	0.004[d]
"	0.84	0.06	0.038	(4)	0.034			
"	"	"				0.019	(4)	0.019[d]
"	0.83	0.07	0.104	(4)	0.019			
"	"	"				0.152	(4)	0.011[e]
"	0.82	0.08	0.152	(4)	0.042			
"	"	"				0.167	(4)	0.038[e]
"	0.81	0.09	0.095	(4)	0.026			
"	0.80	0.10	0.155	(5)	0.053			

[a]CR, carbothermal reduction analysis. [b]AC, acid consumption analysis. [c]Three different experiments. [d]Temperature = 847 °C. [e]Temperature = 878 °C.

Table 2. Solubility of MgO in $MgCl_2$–MgF_2 melts of various compositions at 840 °C.[a]

Melt composition		Oxide content, $x_{MgO}10^3$					
		CR[b]			AC[c]		
x_{MgCl_2}	x_{MgF_2}	Average		SD	Average		±
1.0000	0	6.28	(4)	0.07	6.04	(2)	0.01
1.0000	0	6.02	(3)	0.02	6.01	(2)	0.015
1.0000	0	6.34	(5)	0.43			
0.9979	0.00212	6.29	(5)	0.32			
0.9965	0.00445	6.79	(7)	0.89			
0.9908	0.00923	6.83	(5)	0.75			
0.9757	0.02430	6.27	(4)	0.08			
0.9644	0.03557	6.75	(4)	0.28			
0.9517	0.04830	6.70	(5)	0.07			
0.9333	0.06670	7.69	(5)	1.40			
0.9165	0.08347	6.23	(4)	0.06			
0.9019	0.09806	7.82	(5)	0.11			
0.8844	0.1156	7.68	(5)	0.09			
0.8726	0.1274	7.96	(4)	0.11			
0.8589	0.1411	7.43	(8)	0.15			
0.7984	0.2016	8.14	(5)	1.85			
0.7558	0.2442	8.58	(5)	0.22			
0.7141	0.2859	9.79	(5)	0.06			
0.6010	0.3990	10.9	(5)	0.16			

[a]Number of parallels in parentheses. Standard deviations (SD, ± for AC measurements) reflect the variations between the parallels. [b]CR, carbothermal reduction analysis. [c]AC, acid consumption analysis.

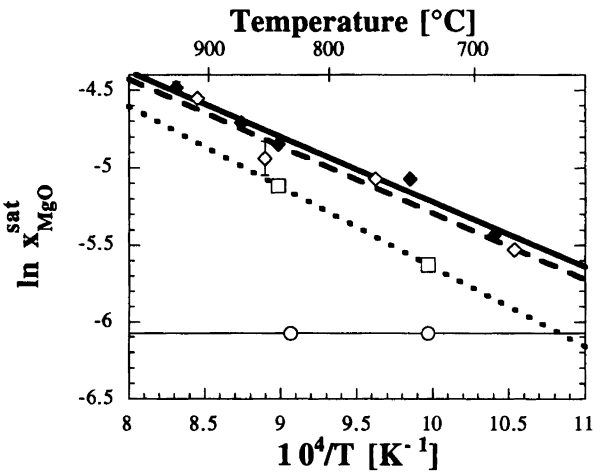

Fig. 8. $\ln x^{sat}_{MgO}$ plotted versus $10^4/T$. (—◆—) $x_{MgF_2}=0.2016$; (—◇—) $x_{MgF_2}=0.1816$; (– –□– –) pure $MgCl_2$; (—○—) NaCl–$MgCl_2$ at $x_{MgCl_2}=0.7$.[18] Lines determined by linear regression.

Table 3. Solubility of MgO in two $MgCl_2$–MgF_2 melts at various temperatures.

$x_{MgF_2}=0.1816$		$x_{MgF_2}=0.2016$	
T/°C	x_{MgO}	T/°C	x_{MgO}
676	0.0040	688	0.0044
766	0.0063	742	0.0063
851	0.0072	840	0.0078
910	0.011	871	0.0090
		930	0.011

nounced, while the system $MgCl_2$–NaCl ($0.42 \leqslant x_{MgCl_2} \leqslant 0.75$) revealed no change in the oxide solubility in the temperature range $475 \leqslant T/°C \leqslant 830$. To understand this variation in the MgO solubility as a function of temperature, let us consider the dissolution reaction for MgO(s):

$$MgO(s) = MgO(l) \quad (2)$$

From tabulated data,[2] the enthalpy of fusion for MgO, $\Delta_{fus}H^\circ_{MgO} = 70 \pm 15$ kJ mol^{-1} at 1000 K. The MgO liquidus line is described by

$$\frac{d(\ln a^{sat}_{MgO})}{d(1/T)} = -\frac{\Delta_{fus}H^\circ_{MgO}}{R} \quad (3)$$

where a_{MgO} is the activity of MgO in the melt using pure liquid MgO as standard state. The enthalpy of fusion of MgO indicates a twofold increase in the activity of MgO(l) for a temperature increase from 730 to 830 °C. The solubility of MgO in $MgCl_2$–NaCl melts, however, is independent of temperature.[18] Our measurements of the MgO solubility in the $MgCl_2$–NaCl eutectic confirmed this observation. The melt was saturated with MgO at 475 °C, and the solubility of MgO was determined to be 0.043 mol%, which is within the uncertainty limits of the data reported by Boghosian *et al.*[18]

Magnesium oxide is probably complexed as $Mg_2OCl_x^{2-x}$ when dissolved in $MgCl_2$-containing melts.[16,18] The complex formation reaction described by eqn. (4)

$$MgO(l) + MgCl_2(l) = Mg_2OCl_2(l) \quad (4)$$

has a large equilibrium constant, i.e. practically all the dissolved oxide is complexed in the melt. Boghosian

et al.[18] concluded that this mechanism was responsible for the MgO dissolution in NaCl–$MgCl_2$ melts for $x_{MgCl_2} > 0.33$. They determined $x^{sat}_{MgO} = 0.0036$ at 730 °C in pure $MgCl_2$, and we have found $x^{sat}_{MgO} = 0.0060$ in the same melt at 840 °C. Both results were obtained using the AC technique.

To explain the above MgO solubility variations let us consider the melt structure of NaCl–$MgCl_2$ melts when the concentration of $MgCl_2$ changes. Raman spectroscopic investigations have shown that discrete tetrahedral $MgCl_4^{2-}$ species are in equilibrium with polynuclear complexes of unknown structure in pure $MgCl_2$.[21] When alkali chlorides are introduced, the scattering from the polynuclear species gradually disappears, and in the basic regimes only the $MgCl_4^{2-}$ complex is present.[22] In other words, $MgCl_2$ changes from a partly ionic, partly network-like melt in the pure state to a typically ionic molten salt when alkali chlorides are introduced.

A system of interest for comparison is the $NdCl_3$–NdOCl system. Pure liquid $NdCl_3$ consists of a network of edge-sharing $NdCl_6^{3-}$ octahedra.[23] The $MgCl_2$–$NdCl_3$ phase diagram indicates close to ideal mixing of the two components.[24] Thus, the two components must be expected to have similar structures in the molten state, or at least that one of the components can be incorporated in the other without altering the structure significantly. In $NdCl_3$ melts, NdOCl have been found to dissolve into the network of edge-sharing $NdCl_6^{3-}$ octahedra, breaking this network down to smaller clusters.[25] We will therefore suggest that MgO dissolves in pure $MgCl_2$ by breaking up the polynuclear complexes of $MgCl_2$, as indicated in the reaction:

$$MgO(s) + [MgCl_2]_n = Mg_{n-m+1}OCl_{2(n-m)} + [MgCl_2]_m \quad (5)$$

$[MgCl_2]_n$ symbolises the polynuclear complexes of unknown structure present in pure $MgCl_2$.[21]

The above considerations indicate that the mechanism for MgO dissolution in pure $MgCl_2$ may be quite different from the mechanism in alkali chloride–$MgCl_2$ melts. This can also be deducted from thermodynamic data.

The activity coefficient of MgO at saturation, γ^{sat}_{MgO}, is given by

$$RT \ln \gamma^{sat}_{MgO} = \Delta \bar{G}^{Ex}_{MgO} = \Delta \bar{H}^{sat}_{MgO} - T\Delta \bar{S}^{Ex}_{MgO} \quad (6)$$

where $\Delta \bar{H}^{sat}_{MgO}$ and $\Delta \bar{S}^{Ex}_{MgO}$ are the partial enthalpy and the excess partial entropy of mixing, respectively, of MgO at the saturation concentration.

At low MgO concentrations it is reasonable to assume that $\Delta \bar{H}^{sat}_{MgO}$ is independent of the MgO solubility. Our data show that $d\ln \gamma^{sat}_{MgO}/d(1/T)$ is a constant for each melt system. By using eqns. (3) and (6) we may therefore determine $\Delta \bar{H}^{sat}_{MgO}$ through the relation

$$\frac{d(\ln x^{sat}_{MgO})}{d(1/T)} + \frac{\Delta_{fus}H^{\circ}_{MgO}}{R} = -\frac{d(\ln \gamma^{sat}_{MgO})}{d(1/T)} = -\frac{\Delta \bar{H}^{sat}_{MgO}}{R} \quad (7)$$

Since the enthalpy of fusion of MgO at the temperature of investigation can be calculated from tabulated thermodynamic data, $\Delta \bar{H}^{sat}_{MgO}$ may be calculated from the straight lines given in Fig. 8. Results are given in Table 4 for $T =$ 1000 K and $\Delta_{fus}H^{\circ}_{MgO} = 70 \pm 15$ kJ mol^{-1}.[2] Within experimental uncertainty $\Delta \bar{H}^{sat}_{MgO}$ is the same in pure $MgCl_2$ and in the two $MgCl_2$–MgF_2 mixtures. The $MgCl_2$–MgF_2 phase diagram indicates that the two components mix ideally. This means that pure MgF_2 as well as the mixture are likely to be structurally similar to $MgCl_2$. Therefore, the MgO dissolution mechanism is expected to be basically the same in MgF_2–$MgCl_2$ melts and in pure $MgCl_2$. This is in agreement with a constant $\Delta \bar{H}^{sat}_{MgO}$. The partial enthalpy of mixing of MgO in the $MgCl_2$–NaCl binary is, however, significantly lower than obtained for $MgCl_2$ and the $MgCl_2$–MgF_2 binary.

The partial enthalpy of dissolution of MgO at the saturation concentration is given by

$$\Delta_{diss}\Delta \bar{H}^{sat}_{MgO} = \Delta_{fus}H^{\circ}_{MgO} + \Delta \bar{H}^{sat}_{MgO} \quad (8)$$

Despite the more positive enthalpy of dissolution in pure $MgCl_2$ than in NaCl–$MgCl_2$ mixtures as can be observed from Table 4, the MgO solubility in NaCl–$MgCl_2$ melts increases with increasing x_{MgCl_2}. This behaviour can be explained by the larger partial excess entropy of mixing of MgO in pure $MgCl_2$ than in the NaCl–$MgCl_2$ mixtures.

From the equilibrium constant of eqn. (2), a^{sat}_{MgO} and eqn. (6), we obtain

$$\lim_{1/T \to 0} R \ln x^{sat}_{MgO} = \Delta_{fus}S^{\circ}_{MgO} + \Delta \bar{S}^{Ex}_{MgO} \quad (9)$$

The partial entropy of dissolution of MgO is, by analogy with eqn. (8), given by

$$\Delta_{diss}\Delta \bar{S}^{sat}_{MgO} = \Delta_{fus}S^{\circ}_{MgO} + \Delta \bar{S}^{id}_{MgO} + \Delta \bar{S}^{Ex}_{MgO} \quad (10)$$

By comparing the variation in $\Delta \bar{S}^{Ex}_{MgO}$ between the systems investigated an explanation for the change in solubility emerges. In Table 4 the left-hand side of eqn. (9) is given for each melt system. From these data we can see that the excess partial entropy of MgO is changing drastically in the positive direction from the NaCl–$MgCl_2$ binary to pure $MgCl_2$. This means that the partial entropy of mixing of MgO in pure $MgCl_2$ is much more positive at a given concentration of MgO than in the NaCl–$MgCl_2$ binary. This entropy change is associated with changes in the solvent. In NaCl–$MgCl_2$ mixtures MgO reacts with an ion in an ionic environment to form a new ion. The melt structure as such is therefore not affected to any significant extent. In pure $MgCl_2$ we have suggested that MgO breaks up $MgCl_2$ clusters with a relatively high degree of local order, and forms smaller ionic species. The dissolution process in $MgCl_2$ is therefore associated with a larger entropy change than the dissolution of MgO in the NaCl–$MgCl_2$ binary. The larger entropy change counteracts the more positive dissolution enthalpy in $MgCl_2$ and results in a higher MgO solubility.

The experimental data of Boghosian *et al.*[18] reveals that a transition in the oxide solubility mechanism in the

Table 4. Partial thermodynamic data of dissolution of MgO(l) in $MgCl_2$, $MgCl_2$–NaCl and $MgCl_2$–MgF_2 melts obtained from the temperature variation of the MgO solubility.[a]

Melt composition							
x_{MgCl_2}	x_{MgF_2}	x_{NaCl}	T/K	Data points	$\frac{d(\ln x^{sat}_{MgO})}{d(1/T)} \Big/ kK$	$\Delta_{diss}\bar{H}^{sat}_{MgO}$/ kJ mol^{-1}, Eqn. (8)	$\lim_{1/T\to 0} R \ln x^{sat}_{MgO}$/ J mol^{-1}, Eqn. (9)
1	0	0	110	2	−5.2	43	−3.8
0.8184	0.182	0	234	4	−4.3	36	−8.1
0.7984	0.202	0	240	5	−4.1	34	−8.5
x^b	0	$1-x^b$	100	3	0	0	−51.0

[a] $\Delta_{fus}H^{\circ}_{MgO}$ *at 1000 K were used in the calculations.*[2] [b] *The data of Boghosian et al.*[18] and the present data for the $MgCl_2$–NaCl eutectic show a temperature independent MgO solubility in the NaCl–$MgCl_2$ system for $0.42 < x_{MgCl_2} < 0.75$, $475 < T/°C < 830$.

NaCl–$MgCl_2$ system occurs in the activity range $0.8 < a_{MgCl_2} < 1$. This was not recognized by these authors due to lack of solubility data as a function of temperature. The idea of a transition region between the partly network-like pure $MgCl_2$(l) and the ionic $MgCl_2$–NaCl mixtures are supported by experimental results obtained by Kisza *et al.*,[26] who found that the exchange current density of magnesium increased when NaCl was added to $MgCl_2$. This indicates that the structural changes taking place in the liquid are more important than the effect of dilution when it comes to the electrochemical activity of $MgCl_2$.

Solubility of MgO and the F^- concentration. An increase in oxide solubility with increasing fluoride content of the melt was expected since the solubility of MgO in MgF_2 is much higher than in $MgCl_2$ (8.5 mol% in MgF_2 at 1228 °C[17] and 0.36 mol% in $MgCl_2$ at 730 °C[18]). The phase diagram for the reciprocal ternary $MgCl_2$–MgF_2–NaCl–NaF system is not known. Owing to the very negative Gibbs energy change for the reaction[2]

$$MgCl_2(l) + 2NaF(l) = MgF_2(l) + 2NaCl(l) \qquad (11)$$

strong negative deviations from ideal mixing for $MgCl_2$ and NaF are expected. It is therefore difficult to estimate ternary melting points accurately. To be sure that our measurements were performed in a one-phase liquid system in equilibrium with MgO(s) we decided to measure the liquidus temperature and the concentrations for one melt which had high NaF and $MgCl_2$ contents. The liquidus temperature for $MgCl_2$(0.63)–NaF(0.20)–NaCl(0.17) was determined to be 620 °C. This indicates that all melts investigated had melting points below the experimental temperature of 850 °C. Furthermore, no tendency for liquid immiscibility was observed at 850 °C. Several melt samples were analysed by Mohr's titration (Cl^-), ion selective electrode (F^-) and ICP (Mg^{2+} and Na^+), and the initial mole fractions of all ions were confirmed. This shows that our solubility data were obtained from a true two-phase system with MgO as the solid phase.

The uncertainties associated with the CR analyses of hygroscopic melt samples add up to about 10% (our best estimate, based on experience). This is considered the most important error source in the saturation mole fraction of MgO, x^{sat}_{MgO}. This uncertainty is indicated in Figs. 4, 5 and 7 as vertical error bars. For the results shown in Fig. 6, however, where the oxide concentrations are very low, the uncertainties in the CR data probably exceed 10%, and we have chosen to adopt the standard deviation between parallels as a measure for the uncertainty in this case. Inaccuracies in temperature and solvent composition are insignificant.

In a NaCl–$MgCl_2$ melt with $x_{MgCl_2} = 0.63$, x^{sat}_{MgO} was determined to be 0.0017[18] in the temperature range $730 < T/°C < 830$. It can be observed from Table 1 that the oxide solubilities determined in the present work differ somewhat from this value. This applies to the results from both oxide analysis techniques. However, while the average taken over all the AC data gives 0.0018, all the CR results yield >0.0027. It was mentioned in the experimental section that problems were experienced during some of the measurements. These problems are reflected in the solubility data for the NaCl–$MgCl_2$ melts. Still, the solubilities determined in the presence of fluoride are well reproduced, as can be observed from Figs. 4 and 5. It is therefore reasonable to assume that the trend in the MgO solubilities as function of fluoride content of the melt is correct.

Figure 2 shows a new peak during the CR analysis when fluoride was introduced to a $MgCl_2$–NaCl mixture. This peak was also observed when MgF_2 was added to $MgCl_2$. This may be attributed to a new oxygen-containing species in mixed chloride–fluoride melts.

To be able to model the oxide solubility in these melts, we have to consider the thermodynamics of these systems. The $MgCl_2$–MgF_2 system behaves ideally, and the activities of the halides can therefore be easily calculated according to the relation $x_{M^{2+}} x^2_{X^-} \gamma_{MX_2}$, where $\gamma_{MX_2} = 1$. It was found that the best fit to the experimental MgO solubilities was obtained with a model described by the equations

$$MgO(s) + MgCl_2(l) = Mg_2OCl_2(l) \qquad (12)$$

$$MgO(s) + \tfrac{1}{2}MgCl_2 + \tfrac{1}{2}MgF_2 = Mg_2OClF(l) \qquad (13)$$

$$MgO(s) + MgF_2(l) = Mg_2OF_2(l) \qquad (14)$$

According to this model, the total MgO solubility in a

given $MgCl_2$–MgF_2 melt should be given by the relation

$$x_{MgO}^{sat} = K_{12}a_{MgCl_2} + K_{13}a_{MgCl_2}^{1/2}a_{MgF_2}^{1/2} + K_{14}a_{MgF_2} \quad (15)$$

where K_{1i} is the equilibrium constant for eqns. (12), (13) and (14). The activities of $MgCl_2$ and MgF_2 are $(x_{MgCl_2})^2$ and $(x_{MgF_2})^2$, respectively. The assumption that the activity coefficients for the oxygen-containing species do not change significantly with melt composition is inherent in the model, and is reasonable in view of the low oxide concentrations observed.

The model has been fitted to the experimental data, and values for the equilibrium constants K_{12}, K_{13} and K_{14} have been obtained. In Fig. 7 it can be seen that the model compares well with experimental data. A model with only two oxygen-containing species, Mg_2OCl_2 and Mg_2OF_2, does not fit the experimental data. It is not surprising, however, that a three-parameter model is able to fit a close to straight line.

Extrapolation of the three-parameter model (solid line in Fig. 7) to $x_{MgF_2}=1$ yields $x_{MgO}^{sat}=0.022$ at $T=840\,°C$. The effect of temperature on the MgO solubility in pure MgF_2 may be estimated using the value for $d(\ln x_{MgO}^{sat})/d(1/T)$ obtained for the $MgCl_2$–MgF_2 ($x_{MgF_2}=0.2016$) mixture. This value is given in Table 4 as $d(\ln x_{MgO}^{sat})/d(1/T)=-4100\,K$. By integration we obtain $x_{MgO}^{sat}=0.057$ in pure MgF_2 at 1228 °C. In view of the approximations applied in our calculation, this must be considered in reasonable agreement with $x_{MgO}^{sat}=0.085$ reported by Sharma.[17]

Activities of salt components for the above $MgCl_2$–NaCl–NaF ternary mixture may be obtained by a model equation developed by Blander[27] based on the work of Førland[28] and Flood *et al.*[29] For the present system the activities of $MgCl_2$ and MgF_2 may be calculated using the equations given in the Appendix. With the data of Kleppa and co-workers[30-33] and Ref. 2 it is possible to calculate the necessary constants in these equations.

We compared this activity model with experimental data in a previous paper.[19] Calculated and measured liquidus lines of the MgX_2-rich sides of the $MgCl_2$–NaCl[34,38] and MgF_2–NaF[35] binaries compared well with the calculations. Calculated and measured activities[36] for the system $MgCl_2$–NaCl also agree within a few percent. We have also made an attempt to calculate the MgF_2 liquidus line of the quasi-binary MgF_2–NaCl system. The model was not in agreement with experimental data.[20] It was mentioned earlier that a liquidus temperature of 620 °C for the melt $MgCl_2(0.63)$–NaF(0.20)–NaCl(0.17) was determined. The model predicts the MgF_2 liquidus temperature to be about 430 °C at this composition. Unless a ternary solid compound is formed, which may be the case, this must be taken as an indication that the model predicts too low values for a_{MgF_2} in melts with low F^- concentrations.

Using eqn. (15) to model MgO solubilities in ternary melts may therefore not be appropriate. In Figs. 4 and 5 we can see that this model equation does not fit with the experimental data.

Conclusion

The present work gives some new insight into the technically important solubilisation mechanism of MgO in $MgCl_2$-containing melts. The temperature effect of the MgO solubility seems to be reasonably well understood. The effect of fluoride concentration on the solubility in the simple $MgCl_2$–MgF_2 binary can also be explained by a reasonable thermodynamic model. When we try to model how MgO dissolves in the $MgCl_2$–NaCl–NaF ternary, however, our concept seems to be too simple. Both the activity model used to calculate a_{MgCl_2} and a_{MgF_2}, and our understanding of the Mg–O–Cl(F) complexes formed in the melt, are too primitive to give a reasonable solubilisation mechanisms of MgO in these complicated melts.

Appendix. Model for calculating activities for the components of the $MgCl_2$–NaCl–NaF reciprocal system

a_{MgCl_2} and a_{MgF_2} have been calculated according to eqns. (A.1) and (A.2).

$$\begin{aligned} a_{MgCl_2} = x_{Mg^{2+}}x_{Cl^-}^2 \exp\Bigg(\frac{1}{RT}[&x'_{Na^+}x_{F^-}\Delta G^\circ_{A.3} \\ &+ 2x_{F^-}(x'_{Mg^{2+}}x_{F^-} + x_{Na^+}x_{Cl^-})\lambda_{Mg}^{eq} \\ &+ 2x'_{Na^+}x_{F^-}(x_{F^-} - x_{Cl^-})\lambda_{Na}^{eq} \\ &+ 2x'_{Na^+}(x'_{Mg^{2+}}x_{F^-} + x'_{Na^+}x_{Cl^-})\lambda_{Cl}^{eq} \\ &+ 2x'_{Na^+}x_{F^-}(x'_{Na^+} - x'_{Mg^{2+}})\lambda_{F}^{eq} \\ &+ 2x'_{Na^+}x_{F^-}(x'_{Na^+}x_{Cl^-} + x'_{Mg^{2+}}x_{F^-} \\ &- x'_{Mg^{2+}}x_{Cl^-})\Lambda^{eq}]\Bigg) \end{aligned} \quad (A.1)$$

a_{MgF_2} = eqn. (A.1), where Cl is exchanged with F and vice versa, and $G^\circ_{A.3}$ is exchanged with $-\Delta G^\circ_{A.3}$. In these equations x_{i^+} and x_{j^-} are cation and anion fractions defined as

$$x_{i^+} = \frac{n_{i^+}}{\sum_i n_{i^+}}$$

and

$$x_{j^-} = \frac{n_{j^-}}{\sum_j n_{j^-}},$$

respectively. The $x'_{Mg^{2+}}$ and x'_{Na^+} are cation equivalent fractions defined as:

$$x'_{Mg^{2+}} = 2n_{Mg^{2+}}/(2n_{Mg^{2+}} + n_{Na^+})$$

and

$$x'_{Na^+} = n_{Na^+}/(2n_{Mg^{2+}} + n_{Na^+})$$

$\Delta G^{\circ}_{A.3}$ refers to eqn. (A.3):

$$NaF(l) + \tfrac{1}{2}MgCl_2(l) = NaCl(l) + \tfrac{1}{2}MgF_2(l) \qquad (A.3)$$

and the λ_i^{eq} are equivalent enthalpy interaction parameters defined for $i = Cl$, F, Mg and Na as

$$\lambda^{eq}_{Cl} = \frac{\Delta H^{m}_{mix}(MgCl_2 - NaCl)}{(1 + x_{Mg^{2+}})} \Big/ x'_{Na^+} x'_{Mg^{2+}}$$

$$\lambda^{eq}_{F} = \frac{\Delta H^{m}_{mix}(MgF_2 - NaF)}{(1 + x_{Mg^{2+}})} \Big/ x'_{Na^+} x'_{Mg^{2+}}$$

$$\lambda^{eq}_{Mg} = [\Delta H^{m}_{mix}(MgCl_2 - MgF_2)/2]/x_{F^-} x_{Cl^-}$$

$$\lambda^{eq}_{Na} = [\Delta H^{m}_{mix}(NaCl - NaF)]/x_{F^-} x_{Cl^-}$$

where ΔH^{m}_{mix} is the molar enthalpy of mixing and

$$\Lambda^{eq} = -\frac{(\Delta G^{\circ}_{A.3})^2}{2ZRT}$$

Z is the cation–anion coordination number.

We have chosen $T = 850\,^{\circ}C$ to compare experimental data with calculation. At this temperature $\Delta G^{\circ}_{A.3} = -77$ kJ, $\lambda^{eq}_{Cl} = -22\,680$ J eq.$^{-1}$, $\lambda^{eq}_{F} = -38\,050$ J eq.$^{-1}$, and $\Lambda^{eq} = -63.502$ kJ eq.$^{-1}$ (using $Z = 5$).[2,30–33] It may be observed from the respective phase diagrams that the systems $MgCl_2$–MgF_2 and NaCl–NaF exhibit close to ideal behavior.[20,37] The numerical values of the respective interaction parameters, λ^{eq}_{Mg} and λ^{eq}_{Na}, therefore, are too small to give significant contributions to a_{MgF_2} and a_{MgCl_2} in the present calculations.

Acknowledgments. Siv.ing. Trond H. Berg carried out the measurements in the $MgCl_2$–MgF_2 system. Financial support from Norsk Hydro and The Norwegian Research Council is greatfully acknowledged. We also want to express our gratitude to O. Wallevik, Norsk Hydro, and to our partners in the Human Capital and Mobility Network under the European Commission for valuable comments and critisism.

References

1. Kannan, G. N. and Desikan, P. S. *Bull. Electrochem. 6* (1990) 776.
2. Chase, M. W., Jr., Davies, C. A., Downey, J. R., Jr., Frurip, D. J., McDonald, R. A. and Syverud, A. N. In Lide, D. R., Jr., Ed. *JANAF Thermochemical Tables, J. Phys. Chem. Ref. Data*, Vol. 14, 3rd edn., American Chemical Society and American Institute of Physics, Washington, DC 1985.
3. Grjotheim, K., Holm, J. L., Lillebuen, B. and Øye, H. A. *Trans. Faraday Soc. 67* (1970) 640.
4. Berge, B., Holm, J. L. and Lillebuen, B. *Acta Chem. Scand. 26* (1972) 257.
5. Grjotheim, K., Nikolic, R. and Øye, H. A. *Acta Chem. Scand. 24* (1970) 489.
6. Dumas, D., Fjeld, B., Grjotheim, K. and Øye, H. A. *Acta Chem. Scand. 27* (1973) 319.
7. Grjotheim, K., Holm, J. L., Lillebuen, B. and Øye, H. A. *Acta Chem. Scand. 26* (1972) 2050.
8. Grjotheim, K., Schultz, A. H. and Øye, H. A. *Metall 26* (1972) 236.
9. Schultz, A. H. and Øye, H. A. *Metall 27* (1973) 252.
10. Anundskås, A., Grjotheim, K., Schultz, A. H., Svendsen, H. and Øye, H. A. *Metall 29* (1975) 493.
11. Anundskås, A., Grjotheim, K., Schultz, A. H., Svendsen, H. and Øye, H. A. *Light Metals 1* (1977) 513.
12. Strelets, K. L. *Electrolytic Production of Magnesium*, Keterpress Enterprises, Jerusalem 1977.
13. Kipouros, G. J. and Sadoway, D. R. *Adv. Molten Salt Chem. 6* (1987) 127.
14. Rao, G. M. *J. Appl. Electrochem. 16* (1986) 626.
15. Wallevik, O. *Personal communication.*
16. Combes, R., de Andrade, F., de Barros, A. and Ferreira, H. *Electrochim. Acta 25* (1980) 371.
17. Sharma, R. A. *J. Am. Ceram. Soc. 71* (1988) 272.
18. Boghosian, S., Godø, A., Mediaas, H., Ravlo, W. and Østvold, T. *Acta Chem. Scand. 45* (1991) 145.
19. Mediaas, H., Vindstad, J. E. and Østvold, T. *Light Metals 20* (1996) 1129.
20. Sharma, R. A. and Johnson, I. *J. Am. Ceram. Soc. 52* (1969) 612.
21. Huang, C. H. and Brooker, M. H. *Chem. Phys. Lett. 43* (1976) 180.
22. Brooker, M. H. and Huang, C. H. *Can. J. Chem. 58* (1980) 168.
23. Photiadis, G., Voyiatzis, G. and Papatheodorou, G. N. *Molten Salt Forum 1–2* (1993/94) 183.
24. Vogel, G. and Schneider, A. *Inorg. Nucl. Chem. Lett. 8* (1972) 513.
25. Mediaas, H., Photiadis, G., Papatheodorou, G. N., Vindstad, J. E. and Østvold, T. *Acta Chem. Scand. 50* (1996). *In press.*
26. Børresen, B., Haarberg, G. M., Tunold, R., Kisza, A. and Kazmierczak, J. *Proceedings of the Tenth International Symposium on Molten Salts*, Electrochem. Soc., Los Angeles 1996.
27. Blander, M. In Mamantov, G. and Marassi, R., Eds., *Molten Salt Chemistry*, Vol. 202, Reidel Publishing Co., Dordrecht 1987, pp. 17–62.
28. Førland, T., In Sundheim, B. R., Ed., *Fused Salts*, McGraw-Hill, London 1964, pp. 63–164.
29. Flood, H., Førland, T. and Grjotheim, K. *Z. Anorg. Chem. 276* (1954) 289.
30. Kleppa, O. J. and McCarty, F. G. *J. Phys. Chem. 70* (1966) 1249.
31. Hong, K. C. and Kleppa, O. J. *J. Phys. Chem. 82* (1978) 1596.
32. Kleppa, O. J. and Melnichak, M. E. In *4th Int. Conf. on Chem. Thermodyn.*, Montpellier, France 1975, pp. 148–156.
33. Kleppa, O. J. In Mamantov, G. and Marassi, R., Eds., *Molten Salt Chemistry*, Vol. 202, Reidel Publishing Co., Dordrecht 1987, pp. 79–122.
34. Grjotheim, K., Holm, J. L. and Rønes, M. *Acta Chem. Scand. 26* (1972) 3802.
35. Bergmann, A. G. and Dergunov, E. P. *C. R. Acad. Sci. URSS 31* (1941) 755.
36. Østvold, T. *High Temp. Sci. 4* (1972) 51.
37. Sangster, J. and Pelton, A. D. *J. Phys. Chem. Ref. Data 16* (1987) 509.
38. Klemm, W. and Weiss, P. *Z. Anorg. Allgem. Chem. 245* (1940) 279.

Received August 28, 1996.